Indian Journal of Chemical Technology
Vol. 31, January 2024, pp. 152-161
DOI: 10.56042/ijct.v31i1.7611

Synthetic layered double hydroxide on biodegradable support: An efficient adsorbent for defluoridation of water

S. Mayadevi [1]*, M. D. Kirandas [1,2], A. M. Manilal [2], Roshini N.[3] & Sujata Mandal[3]*

[1]Chemical Engineering and Process Development Division, National Chemical Laboratory, Pune 411 008, Maharashtra, India
[2]Department of Chemical Engineering, Govt. Engineering College, Trissur 680 009, Kerala, India
[3]Human & Organizational Resources Development, Central Leather Research Institute, Chennai 600 020, Tamil Nadu, India
*E-mail: s.mayadevi@ncl.res.in (S. Mayadevi); sujata@clri.res.in (S. Mandal)

Received 15 March 2023; accepted 12 December 2023

Fluoride concentrations in drinking water above permissible levels and incidences of fluorosis among people have been reported from many parts of the world including India. Low-cost and biodegradable adsorbents are the preferred choice for the removal of fluoride from an aqueous medium. In the present study, zinc-aluminium layered double hydroxide (LDH) supported on sugarcane bagasse (raw and acid-treated) has been synthesized, characterized, and investigated for the defluoridation of water. The SEM micrographs of the supported adsorbents show good dispersion of the LDH particles on the support material. The defluoridation capacity of the LDH is enhanced by supporting it on bagasse. The adsorption capacity of supported adsorbents increased by 3-fold than the unsupported LDH adsorbent. The adsorption data have been well fitted to the Freundlich isotherm model indicating physical and multi-layer adsorption. The maximum fluoride adsorption capacity has been found to be 8.85 mg/g with 76.3% fluoride removal when the initial fluoride concentration is 11-12 mg/L. The pseudo-second-order kinetic model has been found suitable to explain the fluoride adsorption kinetics on the supported LDH adsorbents. The present study reveals that the bagasse-supported LDH adsorbent has a high potential for defluoridation of water.

Keywords: Adsorption kinetics, Fluoride adsorption, Layered double hydroxide, Sugarcane bagasse

Introduction

Fluoride-related health problems, also called fluorosis, are caused by excess intake of fluoride through drinking water over a long period[1,2]. The presence of fluoride in drinking water above the permissible limit is a serious global issue[2,3]. High fluoride concentration in water occurs due to the dissolution of fluoride-containing minerals in the earth's crust. Fluoride-bearing food stuffs and fumes from burning coal also significantly contribute to an increase in fluoride levels in humans. While a low concentration of fluoride in water has beneficial effects on teeth and bones, prolonged excessive intake of fluoride can lead to adverse health effects, ranging from mild dental fluorosis to crippling skeletal fluorosis[2]. The maximum contaminant level of fluoride in drinking water is 1.5 mg/L as per the recommendation by the World Health Organization (WHO)[3]. Higher doses of fluoride interfere with carbohydrates, lipids, proteins, vitamins, enzymes and mineral metabolism and are linked to permanent tooth and skeletal fluorosis in humans[1,2]. Fluoride concentrations in drinking water above permissible levels and incidences of fluorosis have been reported from many parts of the world including Australia, Mexico, Argentina, Egypt, Kenya, UAE, China, Pakistan, Thailand, and India[4–7].

Techniques for the defluoridation of water include chemical precipitation, membrane-based methods, adsorption and ion exchange[1]. The selection of a suitable technique for defluoridation depends on many factors including the concentration of fluoride ions in water, the presence of other ions/contaminants and cost. Adsorption is an efficient method for the defluoridation of water when the fluoride concentration in water is low. Various adsorbents examined for the removal of fluorides from water[8,9] include alumina, bone charcoal, carbonaceous materials, synthetic clays and minerals, industrial waste materials, natural low-cost materials etc.[8,9]. Layered double hydroxides (LDH) are hydrotalcite-like anionic clay materials with positively charged layers composed of bivalent and trivalent metal cations with charge compensating interlayer anions and water molecules[10]. Because of the positively charged metal hydroxide layers and the presence of interlayer exchangeable anions, LDHs are good adsorbents/ion exchangers for anions. During the last two decades,

LDHs have attracted considerable research interest in the environmental field, specifically in water/ wastewater treatment by adsorption/ion exchange and catalytic degradation[11]. LDHs with various bivalent and trivalent combinations have been explored for the removal of various anionic contaminants such as fluoride, arsenic, selenite, phosphate, organic dyes, heavy metals (CrO_4^{2-}, $Cr_2O_7^{2-}$) etc from water[9,11–17]. We had earlier reported that the zinc/aluminium LDH is a good adsorbent for the adsorption of fluoride from water[15,16]. Among the zinc/aluminium LDHs having different zinc: aluminium ratios, the LDH with a ratio of 1:1 was found to have the maximum fluoride adsorption capacity[16]. Since adsorption is a surface phenomenon, supporting the adsorbent on suitable support can increase its dispersion and enhance the adsorption capacity. Mandal and Mayadevi have reported the use of cellulose as the support for LDH adsorbent for the defluoridation of water[18]. Cellulose-supported LDH exhibited fluoride adsorption capacity considerably higher than that of the pristine LDH adsorbent[18]. None other than our previous work has reported the use of such supported LDH adsorbents for the defluoridation of water.

The objective of this study was to prepare zinc/aluminium LDH with enhanced adsorption capacity so that the cost of groundwater purification can be reduced. Zinc/aluminium LDH with Zn:Al molar ratio of 2 (Zn: Al = 2: 1) was used as the active adsorbent in this study. The use of bagasse, an abundant low-cost agro-waste, as support for the active material (LDH) has been examined. Supported adsorbents with three different loadings of the LDH were prepared using raw and acid-modified bagasse as support. Supported adsorbents were characterized for their specific surface area and morphology. Adsorption isotherm and kinetic experiments have been performed to study the defluoridation capacity of the synthesized adsorbents. The performance of the supported LDH adsorbents for the adsorption of fluoride from water has been assessed and compared with other fluoride adsorbents reported in the literature.

Experimental Section

Reagents

Anhydrous aluminium chloride ($AlCl_3$) and zinc chloride ($ZnCl_2$), synthesis grade, were procured from SD Fine-chem Ltd. Sodium fluoride, AR grade, was procured from Merck chemicals. De-ionized water was used for preparing the standard solutions as well as for the syntheses. Sulphuric acid (H_2SO_4), hydrochloric acid (HCl) and orthophosphoric acid (H_3PO_4) used for pre-treatment of the bagasse were LR-grade chemicals procured from SD Fine-chem Ltd.

Adsorbent synthesis

Zn/Al LDH (ZN) was prepared at 60°C by the co-precipitation of an aqueous solution containing the required molar ratio of $ZnCl_2$ and $AlCl_3$ (Zn : Al = 2 : 1) using 2 M NaOH solution, by following the procedure mentioned elsewhere[15,16]. The solution was maintained at a pH of 10±0.5. The precipitate formed was aged for 12 h at 60°C with continuous stirring followed by repeated washing with de-ionized water till the pH of the washing was neutral. The solid mass obtained was then dried at 60°C in an oven under static air till the solid had constant weight. The dried LDH was crushed to a powder form and preserved for further studies. The LDH thus obtained is named ZN.

Bagasse was obtained from a local sugar mill in Pune, India. The collected bagasse was washed thoroughly with water and dried at 60°C in an oven till constant weight was obtained. The dried bagasse consisted of an outer hard layer (mostly crystalline cellulose) with a soft pith in the inner core (mostly amorphous cellulose). The soft inner part was manually separated, triturated using a commercial mixer grinder, sieved using a 25-mesh strainer and used as the support material, hereafter denoted as BPR (Size:> 25-mesh). The sieved raw bagasse (BPR) was pre-treated with different mineral acids before supporting the LDH on it. For pre-treatment, the bagasse (BPR, 5 g each) was dipped in 200 cm^3 0.5 N mineral acid (HCl or H_2SO_4 or H_3PO_4) for two days followed by washing with distilled water till the washing was neutral and dried to constant weight. The HCl, H_2SO_4 and H_3PO_4 treated bagasse thus obtained were denoted as BPHCl, BPH_2SO_4 and BPH_3PO_4, respectively.

For preparing BPR supported LDH with varying loading of LDH, 2 g of BPR was wetted with different quantities of precursor solution ($ZnCl_2$-$AlCl_3$, Zn:Al=2:1) and dried at 45°C for two days with occasional stirring. The dried mass was subsequently wetted with equivalent amounts of 2 M NaOH solution to precipitate the LDH on its surface and kept for 23 days to permit complete precipitation and drying. It was subsequently washed repeatedly with deionised water to remove excess alkali and free LDH particles, and dried at 50°C in an oven. The dried

mass was weighed, and the increase in weight of BPR was noted to calculate the percentage loading of LDH on BPR. Raw bagasse with 28%, 41% and 48% ZN loading were prepared by this method and named as BPR-ZN-28, BPR-ZN-41 and BPR-ZN-48, respectively. The 40% ZN loaded on BPHCl, BPH_2SO_4 and BPH_3PO_4, were also prepared in a similar manner and were designated as BPHCl-ZN-40, BPH_2SO_4-ZN-41 and BPH_3PO_4-ZN-40, respectively.

Characterization techniques

The surface area of the adsorbents was determined by N_2 adsorption-desorption technique using the surface area analyzer, Autosorb 1 from Quantachrome Instruments, USA. The surface morphology of the adsorbents was studied by scanning electron microscopy (SEM, Leica Stereoscan 440 scanning electron microscope).

Batch adsorption experiments

Batch adsorption experiments were conducted in a thermostatic shaker (Julabo SW-21C) at 25°C at the normal pH of the synthetic fluoride solution (pH 6.4 - 6.5) having a concentration between 10 – 50 mg/L. Batch adsorption experiments (adsorbate volume: 50 cm^3; initial concentration: 29.5 mg/L, time: 180 min) with different adsorbent weights (0.02 – 0.3 g) were carried out to optimize the adsorbent dose. An optimized adsorbent dose (0.05 g) was used in all subsequent experiments. Residual fluoride concentration in the filtrate was analyzed by a fluoride ion-selective electrode (ISE, Metrohm 781 pH/Ion Meter). Total ionic strength adjustment buffer (TISAB) was added with the analyte solution in the ratio 1:1 (v/v) during fluoride measurement by ISE. For preparing 100 cm^3 of TISAB solution, 5.84 g NaCl, 5.75 cm^3 glacial acetic acid and 0.45 g CDTA (trans-1,2-diamino-cyclohexane-N,N,N,N-tetraacetic acid monohydrate) was mixed in de-ionized water and made up to 100 cm^3. Samples of fluoride solution were withdrawn at fixed time intervals and analyzed for fluoride concentration. The fluoride adsorption capacity of the adsorbent Q_t (mg/g) at time t (min) was estimated using the formula:

$$Q_t\ (mg/g) = (C_o - C_t) \times V / (W \times 1000) \quad \ldots (1)$$

Here, C_0 and C_t are the concentrations (mg/L) of fluoride at t = 0 and t = t, respectively, V is the volume (cm^3) of fluoride solution and W is the weight (g) of the adsorbent.

Results and Discussion

The adsorbent names, description and their specific surface areas obtained from nitrogen adsorption data at liquid nitrogen temperature are presented in Table 1. The surface area data reveals that raw bagasse does not offer any sites/offer minimum sites for nitrogen adsorption even after treatment with mineral acids. The surface area is the maximum for unsupported LDH, ZN. The surface area of different adsorbents follows the order: ZN >>> BPR-ZN-48 >> BPH_3PO_4-ZN-40 > BPR-ZN-28 > BPHCl-ZN-40 > BPR-ZN-41 ≈ BPH_2SO_4-ZN-41.

The SEM micrographs of BPR, BPR-ZN-41 and BPH_3PO_4-ZN-40 at two different magnifications are presented in Fig. 1. BPR has small flat plate like structure (Fig. 1a) on which the LDH particles are evenly distributed (Fig. 1b). Some small agglomerates of LDH particles are also seen in Fig. 1c. Modification of BPR using H_3PO_4 resulted in smoothening of the flat plates on which the LDH particles are evenly distributed. A comparison of SEM micrographs at two magnifications of BPR and acid modified BPR with LDH loading is presented in Fig. 2. Raw bagasse has an uneven surface. ZN is

Table 1 — Name, description and surface area of the raw and treated supports, and unsupported and supported LDH adsorbents

Sl. No.	Adsorbent name	Description	Surface area (m^2/g)
1	BPR	Raw Bagasse	0.00
2	ZN	Zn-Al LDH, Zn:Al=2:1	62.64
3	BPR-ZN-28	BPR loaded with 28% ZN	8.22
4	BPR-ZN-41	BPR loaded with 41% ZN	5.62
5	BPR-ZN-48	BPR loaded with 48% ZN	17.18
6	BPHCl	BPR treated with HCl	0.00
7	BPH_2SO_4	BPR treated with H_2SO_4	0.00
8	BPH_3PO_4	BPR treated with H_3PO_4	0.39
9	BPHCl-ZN-40	BPHCl loaded with 40% ZN	7.10
10	BPH_2SO_4-ZN-41	BPH_2SO_4 loaded with 41% ZN	5.33
11	BPH_3PO_4-ZN-40	BPH_3PO_4 loaded with 40% ZN	9.782

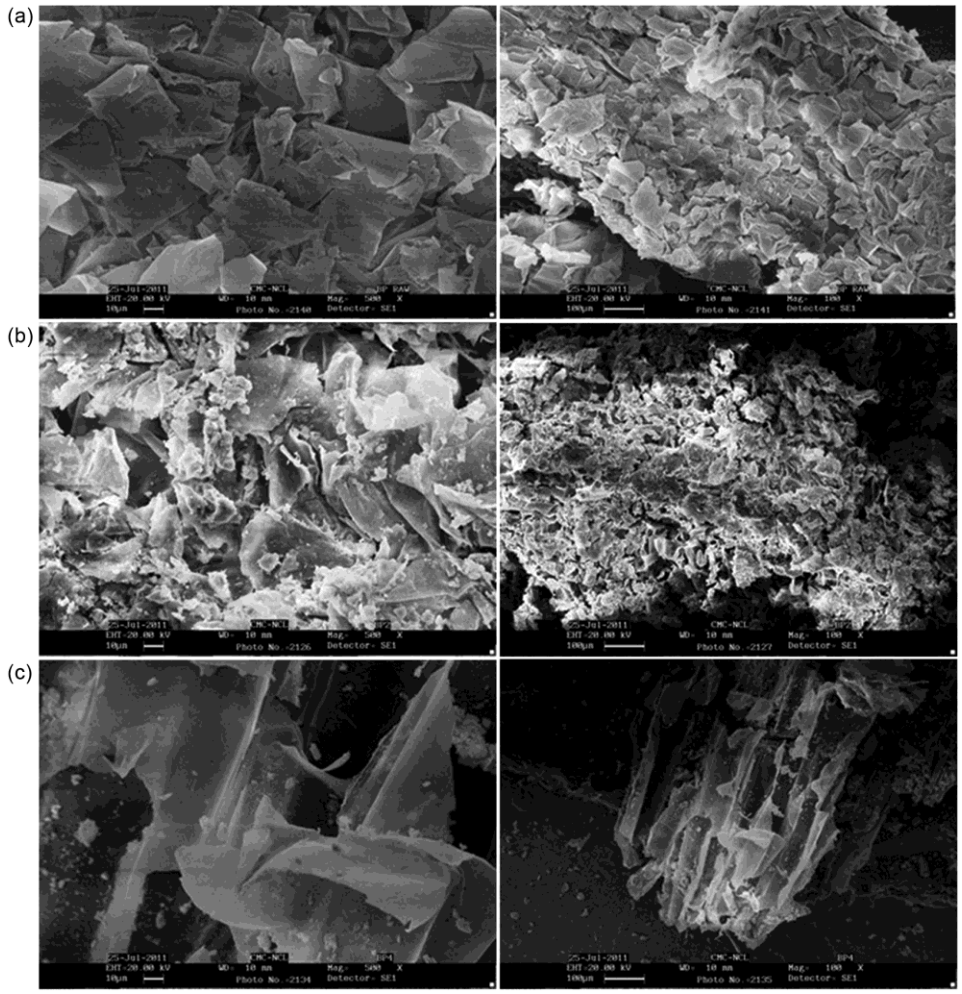

Fig. 1 — SEM micrographs of (a) BPR, (b) BPR-ZN-41 and (c) BPH_3PO_4-ZN-40, at two different magnifications (Left: 500 X and Right: 100 X)

dispersed in a smooth and uniform manner on HCl treated bagasse (2a). Small agglomerates of the LDH can also be noticed on the bagasse surface. ZN dispersion on H_2SO_4 treated bagasse is non-uniform and thick (2c). Larger agglomerates of ZN can also be observed on the surface. The ZN layer on H_3PO_4 modified bagasse is thicker and non- continuous (2d). Presence of ZN agglomerates can also be observed on the surface of supported adsorbent in this sample.

The influence of adsorbent dose on fluoride adsorption (%) by BPR-ZN-41 is presented in Fig. 3, which shows that 0.15 g of the adsorbent is capable of removing more than 90% fluoride from 50 cm^3 (concentration: 29.5 mg/L) of aqueous fluoride solution and 0.3 g of the same adsorbent can remove fluoride almost completely (99.5%) from the solution. An optimized dose of 0.05 g has been used in all further experiments. The optimized adsorbent dose was kept low to record data even at very low initial fluoride concentration.

Variation of adsorption capacity of unsupported LDH (ZN), unsupported adsorbents, supports, and supported adsorbents with time is presented in Fig. 4. The figure reveals that BPR-ZN-41 has higher adsorption rate and higher adsorption capacity compared to the other adsorbents. This is followed by BPR-ZN-48 and BPR-ZN-28. LDH adsorbents loaded on raw bagasse (BPR-ZN-41, BPR-ZN-48 and BPR-ZN-28) show excellent adsorption capacity as compared to those supported on chemically treated bagasse (BP-HCl-ZN-40, BP-H_2SO_4-ZN-41 and BP-H_3PO_4-ZN-40). Raw and chemically modified bagasse supports (BPR, BPHCl, BPH_2SO_4 and BPH_3PO_4) are poor adsorbents for the adsorption of fluoride ions. Fig. 4 shows that the maximum adsorption occurs at the contact time of 60 min. For most of the adsorbents, equilibrium adsorption has

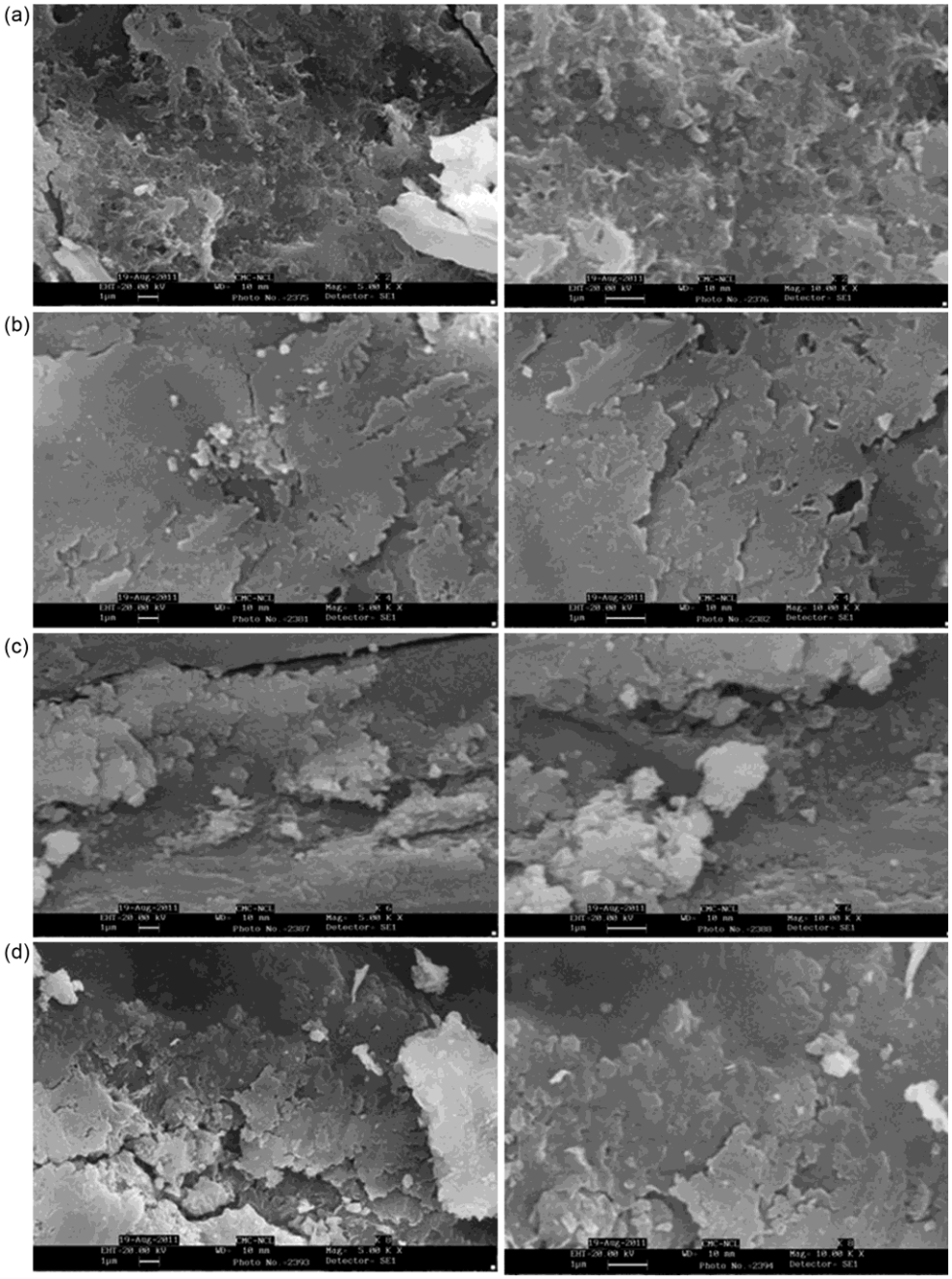

Fig. 2 — SEM micrographs of LDH loaded (a) BPR, (b) BPHCL-ZN-40, (c) BPH_2SO_4-ZN-41 and (d) BPH_3PO_4-ZN-40, at two different magnifications (Left: 5 X and Right: 10 X)

been achieved within 60 min of adsorption. However, in case of adsorbents having very high adsorption capacity, fluoride ions start desorbing very slowly after the maximum adsorption capacity has been reached (C_t>60 min).

It is observed that those adsorbents having very low surface area exhibit poor adsorption behaviour towards the adsorption of fluoride ions. This is to be expected as adsorption is a surface phenomenon. The raw and acid treated bagasse (BPR, BPHCl, BPH_2SO_4 and BPH_3PO_4) do not offer any sites for nitrogen adsorption during surface area analysis (Table 1) and hence show very low fluoride adsorption capacity. All the supported LDH adsorbents show surface area within the range 5 – 17 m^2/g, which is very less as compared to that of the unsupported LDH, ZN (62.64 m^2/g). However, the fluoride adsorption capacity of the adsorbents, BPR-ZN-41, BPR-ZN-48

and BPR-ZN-28, show a three-fold increase as compared to that of the unsupported LDH (ZN). The very high adsorption capacity of the supported LDH adsorbents in spite of low specific surface area may be attributed to the higher dispersion of active LDH particles providing more active surface sites for the adsorbate (fluoride) ions. Because of the very high fluoride adsorption capacity of the supported LDH adsorbents, BPR-ZN-41, BPR-ZN-48 and BPR-ZN-28, they are selected for further detailed study.

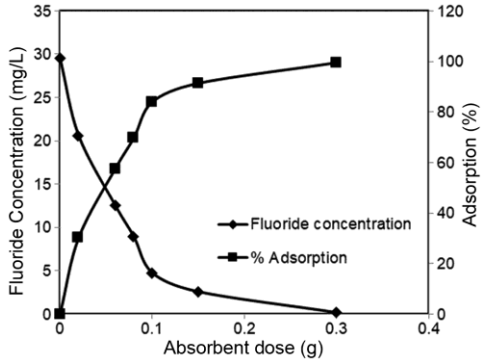

Fig. 3 — Influence of adsorbent dose on fluoride adsorption (%) and equilibrium fluoride concentration for the LDH loaded bagasse, BPR-ZN-41 (volume of adsorbate: 50 cm^3, contact time: 180 min, temperature: 25°C)

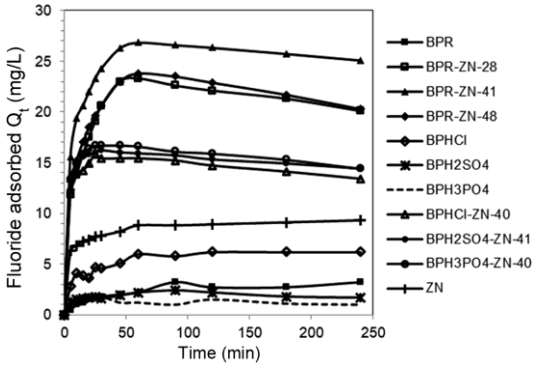

Fig. 4 — Variation of fluoride adsorption capacity of the adsorbents as a function of time (volume of adsorbate: 50 cm^3, initial fluoride concentration: 30 mg/L, weight of adsorbent: 0.05 g, temperature: 25°C)

The adsorption kinetic data for the supported and unsupported LDH adsorbents, BPR-ZN-41, BPR-ZN-48, BPR-ZN-28, BP-HCl-ZN-40, BP-H_2SO_4-ZN-41, BP-H_3PO_4-ZN-40 and ZN, are fitted to the first order and pseudo second order kinetic equations. Lagergren first order kinetic model used for the kinetic analysis is presented below[19].

$$\ln (Q_e\text{-}Q_t) = \ln Q_e - k_1 t \quad \text{... (2)}$$

where, Q_e is equilibrium adsorption capacity, Q_t is adsorption capacity at time t and k_1 is the first order rate constant.

The pseudo second order kinetic equation as proposed by Ho and Mckay[20] is presented below:

$$\frac{t}{Q_t} = \frac{1}{k_2 Q_e^2} + \frac{t}{Q_e} \quad \text{... (3)}$$

where, Q_e and Q_t have the same meaning as described earlier, and k_2 is the second-order rate constant.

The adsorption data up to 60 min of contact time have been taken for kinetic analysis as a slight decrease in adsorption capacity (due to desorption of fluoride ions) is observed, at C_t> 60 min in Fig. 4, for all the three selected adsorbents.

The first order and second order rate constants (k_1 and k_2) and adsorption capacities calculated from the slope and intercept of the linearized plot of Eqs 2 and 3 along with the corresponding correlation coefficients (R^2) are presented in Table 2. The untreated supported adsorbents (BPR-ZN-41, BPR-ZN-48 and BPR-ZN-28) have much higher fluoride adsorption capacities than those for the acid-treated supported adsorbents (BP-HCl-ZN-40, BP-H_2SO_4-ZN-41 and BP-H_3PO_4-ZN-40) and the unsupported LDH (ZN). However, the rates of adsorption are very fast in case of acid-treated supported adsorbents (BP-HCl-ZN-40, BP-H_2SO_4-ZN-41 and BP-H_3PO_4-ZN-40) than those for untreated supported adsorbents (BPR-ZN-41, BPR-ZN-48 and BPR-ZN-28), as indicated by the rate constant values (k_1 and k_2). The

Table 2 — First-order and pseudo-second-order rate constants, correlation coefficients and the adsorption capacities of the supported and unsupported LDH adsorbents

Adsorbent	$Q_{e(exp)}$ mg/g	First-order kinetic parameters			Pseudo-second-order kinetic parameters		
		k_1 (1/min)	R^2	$Q_{e(cal)}$ (mg/g)	k_2 (g/mg.min)	R^2	$Q_{e(cal)}$ (mg/g)
BPR-ZN-28	23.30	0.079	0.973	23.88	0.004	0.993	27.03
BPR-ZN-41	26.84	0.09	0.954	25.41	0.006	0.998	29.41
BPR-ZN-48	23.80	0.082	0.943	25.03	0.004	0.996	27.03
BPHCl-ZN-40	15.80	0.219	0.974	12.06	0.058	0.999	15.87
BPH_2SO_4-ZN-41	16.20	0.118	0.905	8.08	0.095	0.999	16.39
BPH_3PO_4-ZN-40	16.7	0.186	0.971	13.30	0.055	0.999	17.24
ZN	9.30	0.035	0.833	4.66	0.028	0.996	9.17

values of correlation coefficients (R^2) presented in Table 2 clearly indicate better fitting of the pseudo second order kinetic model than the first order kinetic model. Adsorption capacities at different contact times have been calculated [Q_t (cal)] for each adsorbent using the rate constants (k_1 / k_2) and Q_e values, presented in Table 2, individually using first- and second-order kinetic models (Eqs 2 and 3). Plots for experimental adsorption capacities versus calculated adsorption capacities [Q_t (exp) versus Q_t (cal)] obtained using first-order and pseudo-second-order kinetic models have been presented as Fig. 5 and Fig. 6, respectively. A fairly good agreement between the Q_t (cal) and Q_t (exp) values can be observed in Fig. 6. A comparison of Fig. 5 and Fig. 6 clearly indicate that the pseudo-second-order kinetic model can be taken as the best model to explain the kinetics of fluoride adsorption on the selected supported LDH adsorbents.

Adsorption equilibrium data for the adsorption of fluoride on the three selected supported LDH adsorbents are fitted to the Langmuir[21] and Freundlich[22] isotherm models. Adsorption equilibrium data gave a poor fit to the Langmuir adsorption model (not presented). The data for all three adsorbents fitted reasonably well with the Freundlich isotherm model (Eq. 4).

$$Q_e = k_F C_e^{1/n} \quad \text{... (4)}$$

where, k_F and n are Freundlich constants characteristics of the system representing, adsorption capacity and adsorption intensity, respectively. A linearized form of Eq. 4 can be written as follows.

$$\ln Q_e = lnk_F + \frac{1}{n} lnC_e \quad \text{... (5)}$$

The Freundlich constants k_F and n are calculated respectively from slope and intercept of the straight line obtained from the plot of $\ln k_F$ versus $\ln Q_e$. Table 3 shows the values of Freundlich constants and their corresponding correlation coefficients.

The predicted values of equilibrium adsorption capacities [Q_e (pred)] for each adsorbent are calculated by substituting the values of Freundlich constants 'k_F' and 'n' in Eq. 4. Parity plot of experimental Q_e versus that calculated using the Freundlich model for all the selected supported and unsupported LDH adsorbents is presented as Fig. 7. Fig. 7 shows that the data are clustered around the trend line corresponding to Q_e (exp) = Q_e (pred) indicating that this model can be used for predicting the equilibrium behaviour of the adsorbents for fluoride adsorption in an aqueous medium. The value of the constant 'n' which represents adsorption intensity, is much higher than unity (except for BPR-ZN-28) suggesting that fluoride adsorption is highly favoured on these adsorbents. However, the calculated values of Freundlich constant 'k' are much lower than the experimentally obtained adsorption capacities of the adsorbents. A better fitting of the adsorption data in the Freundlich isotherm model than the Langmuir isotherm model indicates that the adsorption of fluoride ions on the supported LDH adsorbents is purely physical in nature. The

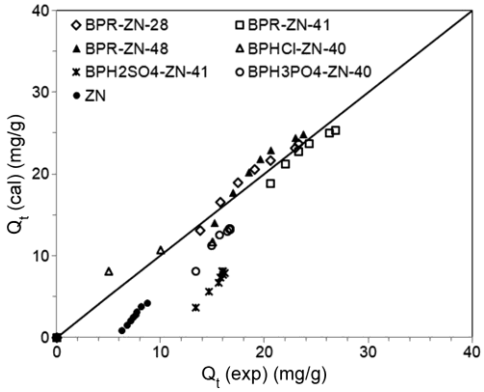

Fig. 5 — Plot of Q_t (exp) vs Q_t (cal) obtained using Lagergren pseudo first order kinetic equation (t = 0 to 60 min)

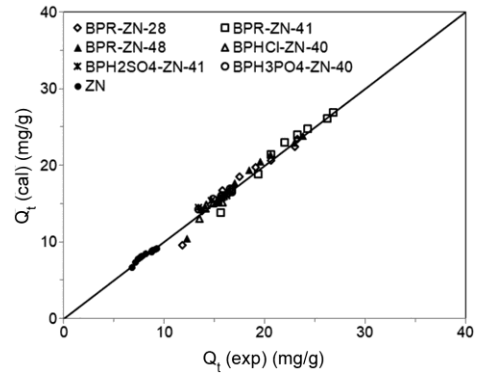

Fig. 6 — Plot of Q_t (exp) vs Q_t (cal) obtained using pseudo second order kinetic model proposed by Ho and Mckay (t= 0 to 60 min)

Table 3 — Freundlich isotherm constants and the corresponding correlation coefficients for the supported and unsupported LDH adsorbents

Adsorbent	n	k_F	R^2
BPR-ZN-28	0.81	0.79	0.774
BPR-ZN-41	1.57	6.02	0.729
BPR-ZN-48	1.27	4.78	0.894
BPHCl-ZN-40	5.08	7.61	0.742
BPH_2SO_4-ZN-41	4.12	7.99	0.860
BPH_3PO_4-ZN-40	4.52	8.36	0.994
ZN	1.24	1.82	0.711

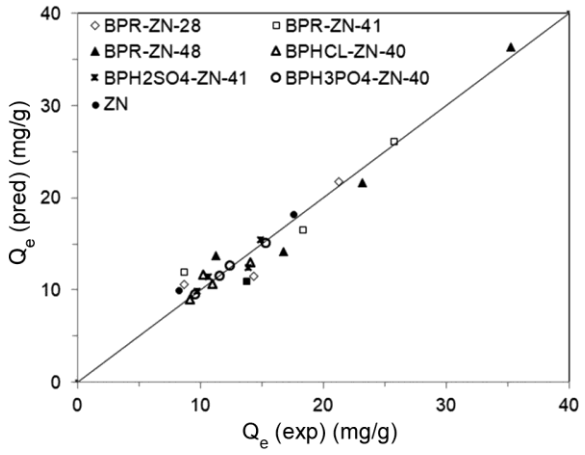

Fig. 7 — Parity plot of experimental adsorption capacity [Q_e (exp)] versus that predicted [Q_e (pred)] using the Freundlich isotherm model for the adsorption of fluoride ions on different supported and unsupported adsorbents

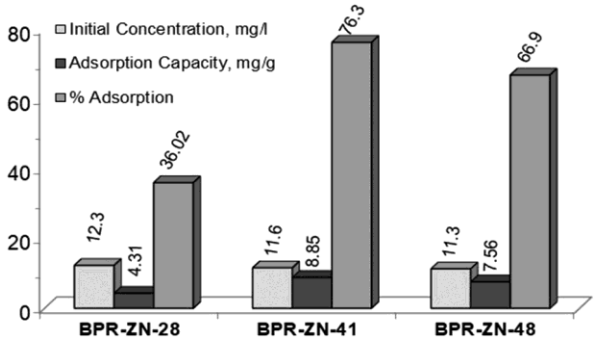

Fig. 8 — Fluoride adsorption capacity and the corresponding adsorption percentage of the supported adsorbents at low initial fluoride concentrations (weight of the adsorbent: 0.05 g, volume of adsorbate: 50 cm^3, contact time: 120 min, temperature: 25°C)

Freundlich isotherm model also assumes multilayer adsorption on an energetically heterogeneous surface having surface sites with a varying affinity for the adsorbate. In the present case, the supported LDH adsorbent contains both LDH (the active material) and support material on its surface, which provide energetically different surface sites for the fluoride ions.

The concentrations of Fluoride ions in contaminated water usually lie below 5 mg/L. Hence, the adsorption experiments are performed at low initial fluoride concentrations using the synthesized bagasse-supported LDH adsorbents. Fig. 8 shows the fluoride adsorption capacities, and adsorption percentages of the selected three supported LDH adsorbents when the initial fluoride concentration in water is between 11-12 mg/L. It can be observed that among the three adsorbents, BPR-ZN-41 is the best-performing adsorbent having an adsorption capacity of 8.85 mg/g with 76.3% fluoride removal. Complete removal of fluoride is possible by increasing the adsorbent dose. It is possible to bring down the fluoride concentration below the MCL (1.5 mg/L) recommended by WHO, by using an appropriate adsorbent dose.

The fluoride removal performance of the synthesized supported LDH adsorbents is compared with that of the adsorbents available in the literature. Bhatnagar et al., have reviewed and listed fluoride adsorption capacities of different adsorbents available in the literature up to the year 2011[8]. Research articles on the defluoridation of water by adsorption, published after 2011 till date, have also been reviewed for the defluoridation capacity of the reported adsorbents. Adsorbents having high defluoridation capacities are presented in Table 4 along with that of the bagasse-supported LDH adsorbent (from the present study). Table 4 shows that the defluoridation capacity of the synthesized supported adsorbent is higher than that of impregnated and activated alumina adsorbents in both low and medium fluoride concentrations. However, some nano-sorbents show better defluoridation capacity than the bagasse supported LDH adsorbent. Since the bagasse supported LDH adsorbent is low-cost and bio-degradable, it is more advantageous than nano-sorbents. The fluoride adsorption capacities of cellulose supported Zn/Al LDH[18]and sodium alginate – Mg/Al composites[23], reported previously by our research group, are 13.8 mg/g and 5.2 mg/g, respectively. The bagasse supported LDH adsorbents show much higher fluoride uptake as compared to that of the cellulose supported LDH and sodium alginate – Mg/Al composites.

The reusability potential of any adsorbent is an important factor for its commercial application. The regeneration and reuse of the adsorbents depends on the desorption of the adsorbate from the adsorbent under the influence of a stimuli such as chemical, temperature, etc. Though desorption of the fluoride from the supported LDH adsorbents have not been studied however, as per the reported literature, dilute solution of NaOH (0.01 – 0.1 M) will be suitable for desorption of fluoride ions from the LDH adsorbent[15,35]. The concentration of the NaOH solution may be fixed depends on the fluoride loading on the adsorbent.

Table 4 — A comparison of the fluoride removal performance of the synthesized supported LDH adsorbents with that of the adsorbents available in the literature

Sl. No.	Adsorbent	Initial fluoride conc. (mg/L)	Adsorption capacity (mg/g)
1	MnO_2 modified activated alumina[8]	10.0	4- 5
2	Nano goethite[8]	30	17-18
3	Schwertmannite[8]	10	7.9
4	Quick lime[8]	10-50	16.67
5	CuO-coated alumina[8]	10	7.77
6	Al-Ce hybrid adsorbent[8]	2-15	91.4
7	Glutaraldehyde cross-linked calcium alginate (GCA)[8]	10-25	73.6
8	Calcined Zn/Al hydrotalcite like compound[8]	10	13.43
9	CaO nanoparticles[8]	10-100	163.3
10	Nano-magnesia[8]	5-200	267.82
11	Fe_3O_4 on $Al(OH)_3$ NPs[8]	0-160	88.48
12	KMnO4 modified carbon[8]	20	15.9
13	Zirconium - iron oxide[8]	10	9.8
14	Fe-Tinano oxide[24]	50	29.85
15	Li-Al Layered double hydroxides[25]	200	42.43
16	Bio-char from Pine wood and Pine bark[26]	1-100	6-8.5
17	Carboxylated aerobic granules containing Ce(III)[27]	4-20	45
18	Sodium alginate – Mg/Al composite[23]	10	5.2
19	Cellulose supported LDH[18]	50	13.80
20	Raw laponite[28]	5-20	10.8
21	Aluminium hydroxide impregnated sawdust[29]	5-30	4.45
22	UiO-66-NH_2@PS^+ composite[30]	5-80	27.5, 32.8
23	Cockle (Anadaragranosa) shells-based hydroxyapatite[31]	10-80	15.374
24	Aluminium (Al^{3+}) fabricated 2-aminobenzene-1,4-dicarboxylic acid (ABDC) namely Al@ABDC metal organic frameworks (MOFs)[32]	--	4.9
25	Diatomite Modified with Aluminium hydroxide[33]	10	1.67
26	Ion channel modified Hydroxyapatite[34]	5	1.56-2.34
27	BPR-ZN-41[#]	10-12	8.85
28	BPR-ZN-41[#]	30-35	26.34

Conclusion

Zinc-aluminium LDH was supported on sugarcane bagasse, which is a biodegradable waste material. SEM micrographs revealed that the LDH is highly dispersed on the support surface. Among all the adsorbents, LDH supported on untreated/raw bagasse showed maximum defluoridation capacities and followed the order BPR-ZN-41 > BPR-ZN-48 > BPR-ZN-28. The higher adsorption characteristic of the supported adsorbents has been attributed to the better dispersion of the active adsorbent (LDH) on the support. The adsorption equilibrium data could be well explained using the Freundlich isotherm model, which assumes purely physical - multilayer adsorption. The Freundlich isotherm constant 'n' was higher than unity signified favourable conditions for the adsorption of fluoride ions on supported LDH adsorbents. The adsorption kinetic followed the pseudo-second-order kinetic model. The equilibrium adsorption capacities calculated using the pseudo-second-order kinetic model match well with the corresponding experimental values. The adsorption capacity of the supported adsorbents was much higher than that of the impregnated and activated alumina adsorbents even at very low fluoride concentrations. As bagasse is biodegradable, non-toxic, and easily available waste material, its use as support in the defluoridation of water can bring down the adsorbent cost and increase the ease of environment-friendly disposal of the used adsorbent.

Acknowledgement

RN acknowledges the financial support received from the project NWP0100.

References

1 Ahmad S, Singh R, Arfin T & Neeti K, Fluoride contamination, consequences and removal techniques in water: A review, *Environ Sci Adv*, 1 (2022) 620.

2 Fawell J, Bailey K, Chilton J, Dahi E, Fewtrell L & Magara Y, Flouride in Drinking-water, *World Health Organization*, IWA Publishing, UK (2001).

3 WHO Guidelines for drinking-water quality [electronic resource] : incorporating first addendum, Recommendations, 3rd ed. World Health Organization. https://apps.who.int/iris/handle/10665/43428. World Health Organization. Water, Sanitation and Health Team 1 (2006).

4 Mandinic Z, Curcic M, Antonijevic B, Lekic C P & Carevic M, Relationship between fluoride intake in Serbian children living in two areas with different natural levels of fluorides and occurrence of dental fluorosis, *Food Chem Toxicol*, 47 (2009) 1080.

5 Amini M, Fawell J, Bailey K, Chilton J, Dahi E, Fewtrell L & Magara Y, Statistical modeling of global geogenic fluoride contamination in groundwaters, *Environ Sci Technol*, 42 (2008) 3662.

6 Tekle-Haimanot R, Melaku Z, Kloos H, Reimann C, Fantaye W, Zerihun L & Bjorvatn K, The geographic distribution of fluoride in surface and groundwater in Ethiopia with an emphasis on the Rift Valley, *Sci Total Environ*, 367 (2006) 182.

7 Reardon E J & Wang Y, A Limestone Reactor for Fluoride Removal from Wastewaters, *Environ Sci Technol*, 34 (2000) 3247.

8 Bhatnagar A, Kumar E & Sillanpää M, Fluoride removal from water by adsorption-A review, *Chem Eng J*, 171 (2011) 811.

9 Mandal S & Mayadevi S, In: Fluoride: Properties, Applications and Environmental Management, *Nova Publishers Inc., New York*, (2011) 159.

10 Sahoo D P, Das K K, Mansingh S, Sultana S & Parida K, Recent progress in first row transition metal Layered double hydroxide (LDH) based electrocatalysts towards water splitting: A review with insights on synthesis, *Coord Chem Rev*, 469 (2022) 214666.

11 Dong Y, Kong X, Luo X & Wang H, Adsorptive removal of heavy metal anions from water by layered double hydroxide, *A Rev Chemosphere*, 303 (2022) 134685.

12 Das D P, Das J & Parida K, Physicochemical characterization and adsorption behavior of calcined Zn/Al hydrotalcite-like compound (HTlc) towards removal of fluoride from aqueous solution, *J Colloid Interface Sci*, 261 (2003) 213.

13 Das J, Patra B S, Baliarsingh N & Parida K M, Adsorption of phosphate by layered double hydroxides in aqueous solutions, *Appl Clay Sci*, 32 (2006) 252.

14 Mandal S, Mayadevi S & Kulkarni B D, Adsorption of aqueous selenite [Se(IV)] species on synthetic layered double hydroxide materials, *Ind Eng Chem Res*, 48 (2009) 7893.

15 Mandal S & Mayadevi S, Defluoridation of water using as-synthesized Zn/Al/Cl anionic clay adsorbent: Equilibrium and regeneration studies, *J Hazard Mater*, 167 (2009) 873.

16 Mandal S & Mayadevi S, Adsorption of fluoride ions by Zn-Al layered double hydroxides, *Appl Clay Sci*, 40 (2008) 54.

17 Mandal S, Natarajan S, Raja S, Vijayalakshmi N, Muralidharan C & Mandal A, Adsorption of Acid Dyes on Hydrotalcite-Like Anionic Clays, *Key Eng Mater*, 571 (2013) 57.

18 Mandal S & Mayadevi S, Cellulose supported layered double hydroxides for the adsorption of fluoride from aqueous solution, *Chemosphere*, 72 (2008) 995.

19 Lagergren S, About the theory of so-called adsorption of soluble substance, *Handlingar*, 24 (1989) 1.

20 Ho Y, The kinetics of sorption of divalent metal ions onto sphagnum moss peat, *Water Res*, 34 (2000) 735.

21 Langmuir I, The adsorption of gases in plane surface of glass, mica, and platinum, *J Am Chem Soc*, 40 (1916) 1361.

22 Freundlich H M F, Over the adsorption in solution, *J Phys Chem*, 385 (1906) 385.

23 Mandal S, Patil V S & Mayadevi S, Alginate and hydrotalcite-like anionic clay composite systems: Synthesis, characterization and application studies, *Micropor Mesopor Mater*, 158 (2012) 241.

24 Chen L, Shuai H, Bo-Yang H, Ting-Jie W, Chao-Li S, Chang Z & Yong J, Synthesis of iron-doped titanium oxide nanoadsorbent and its adsorption characteristics for fluoride in drinking water, *Ind Eng Chem Res*, 51 (2012) 13150.

25 Zhang T, Li Q, Xiao H, Lu H & Zhou Y, Synthesis of Li-Al layered double hydroxides (LDHs) for efficient fluoride removal, *Ind Eng Chem Res*, 51 (2012) 11490.

26 Mohan D, Sharma R, Singh V K, Steele P & Pittman C U, Fluoride removal from water using bio-char, a green waste, low-cost adsorbent: Equilibrium uptake and sorption dynamics modeling, *Ind Eng Chem Res*, 51 (2012) 900.

27 Wang X H, Song R H, Yang H C, Shi Y J, Dang Y G, Yang S, Zhao Y, Sun X F & Wang S G, Fluoride adsorption on carboxylated aerobic granules containing Ce(III), *Bioresour Technol*, 127 (2013) 106.

28 Braik S, Amor T B, Michelin L, Rigolet L, Bonne M, Lebeau B & Hafian A, Natural water defluoridation by adsorption on Laponite clay, *Water Sci Technol*, 85 (2022) 1701.

29 Mandal S, Johri S & Govind M, Aluminium hydroxide impregnated sawdust adsorbent: An eco-friendly and low-cost strategy for defluoridation of water, *Indian J Chem Technol*, 29 (2022) 139.

30 Ni W, Dai H, Ding G, Ye M & Qiu H, Effective defluoridation of water using nanosized UiO-66-NH_2 encapsulated within macroreticular polystyrene anion exchanger, *Chemosphere*, 300 (2022) 134584.

31 Mtavangu S G, Mahene W, Machunda R L, van der Bruggen B & Njau K N, Cockle (Anadara granosa) shells-based hydroxyapatite and its potential for defluoridation of drinking water, *Results Eng*, 13 (2022) 100379.

32 Jeyaseelan A, Kumar I A, Viswanathan N & Naushad M, Rationally designed and hierarchically structured functionalized aluminium organic frameworks incorporated chitosan hybrid beads for defluoridation of water, *Int J Biol Macromol*, 207 (2022) 941.

33 Akafu T, Chimdi A & Gomoro K, Removal of fluoride from drinking water by sorption using diatomite modified with aluminum hydroxide, *J Anal Methods Chem*, 2019 (2019) 4831926.

34 Huang S, Zhang X,Wang L, Li D, Zhang C, Yang L, He Q & Bin G B, Enhanced water defluoridation using ion channel modified hydroxyapatite: Experimental, mechanisms and DFT calculation, *Appl Surf Sci*, 615 (2023) 156351.

35 Li Y, Narducci R, Varone A, Kaciulis S, Bolli E & Pizzoferrato R, Zn–Al layered double hydroxides synthesized on aluminum foams for fluoride removal from Water, *Processes*, 9 (2021) 2109.